DESIGN AND ANALYSIS OF A LIQUID DESICCANT DEHUMIDIFIER

P. Raja Naveen[1] , G. Ramakrishna [2], N.S.C.Chaitanya[3]

Associate Professor ,Mechanical Engineering, Raghu Engineering College(Autonomous),Vishakhapatnam[1,3]
Assistant Professor ,Mechanical Engineering,Raghu Engineering College(Autonomous),Vishakhapatnam[2]

ABSTRACT

Increasing of occupant comfort demands are leading to rising requirement for air conditioning, but deteriorating global energy and environment crisis are starving for energy saving and environmental protection. The need to come up with the new energy saving as well as environmental friendly air conditioning systems has been more urgent than ever before.

In hot and humid areas, the liquid desiccant air-conditioning systems based on evaporative cooling was proposed as an alternative to the traditional vapor compression systems due to its advantage in, removing the air latent load, friendly to environment, removing of pollutants from the process air and reduction of the electrical energy. In this project, recent researches and development activities in liquid desiccant dehumidification systems combined with evaporative cooling technologies are surveyed.

Following that\, such a liquid dehumidifier is fabricated. In this system, CaCl2 salt solution is used for dehumidification of air. Strong solution is internally cooled to minimize heating up of the solution which causes reduction in its absorbing capacity. Evaporative cooling that follows is more effective because dehumidified air flows over cooling water spray. Weak solution is regenerated by an electric heater. Finally air gets cooled and dehumidified. Heating for regeneration can be done using any cheap heat source like waste heat, solar energy.

Direct evaporative cooling gives good effect in dry areas. Its effectiveness is not much in humid areas. To be suitable for such high humidity conditions in this system air is dried first using cacl2 salt solution. Heat is generated during dehumidification. Cooling water is circulated to absorb this heat. Evaporative cooler also cools the salt solution after it got regenerated by heating.

Keywords: Dehumidification systems, air-conditioning systems, CaCl2 salt solution etc.

I.INTRODUCTION

Liquid desiccants are solutions that have a high affinity for water vapor. This property is the key to creating cooling systems that dehumidify air without over-cooling. (Dr. Lowenstein's review paper presents a more detailed explanation of the theory, operation and status of liquid desiccant air conditioners than can be included here.)

Since the 1930s, liquid desiccants have been used in industrial dehumidifiers. The liquid desiccants used in these systems commonly are very strong solutions of the ionic salts lithium chloride and calcium chloride. These ionic salts have the attractive characteristic that the salts themselves have essential zero vapor pressure, and so vapors of the desiccant will not appear in the air supplied by the liquid desiccant air conditioning . However, zero vapor pressure comes with a price: as with seawater (a chemically similar salt solution), solutions of lithium and calcium chloride are very corrosive. This corrosiveness requires that all wetted parts within the liquid desiccant air conditioning be protected and that no droplets of desiccant are entrained by the supply air.

1.1 SIMULATION METHODOLOGY:

The simplified geometric construction of a dehumidifier is presented in Fig. 1, whose size is 150 mm _ 10 mm. The simulation is conducted for the unsteady two-phase flow with free liquid surface in the channel between two flat plates. The liquid desiccant solution is supplied from the upper-left hole to the duct while the moist air introduced by the bottom-right hole. In this way, the liquid and gas flow counter-currently. The gravity is considered in the simulation. The point at the bottom-left corner is set as the origin (0, 0) of the orthogonal coordinate.

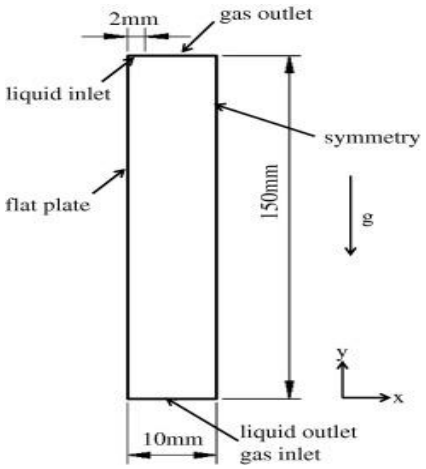

Figure 1.1 Schematic diagram of simplified physical model

The PAM has a thin-walled, rubber bladder placed inside an axially stiff but radically compliant braided sleeve. As the rubber bladder expands due to an increase in pressure, the diameter of the combined sleeve and bladder assembly easily changes in the radial direction and the PAM shortens in the axial direction. As the consequence of this interaction, a large contraction force produced can perform external work at rapid rate. However, non-linearity exists as the pressure changes in the bladder because its area expands proportionally to the square of the diameter.Also as the outer sheath material moves, its length is dependent on trigonometric relationships involving the outer sheath material, which are non-linear. Thus this displacement is used to actuate a link.

1.2. MESHING AND SOLUTION SCHEME

In the simulation, the flow field is meshed by the structured grid. Four grids are adopted for the independence study: 49 _ 250, 71 _ 300, 71 _ 500, and 81 _ 500. As a result of the thin thickness of the liquid film, the grid density increases gradually from the gas to the liquid phase. In the x direction, the grid that near the wall has the smallest size (0.04–0.1 mm), and the grid near the symmetry possesses the largest size (0.2–0.3 mm). In the y direction, a uniform grid is employed with sizes 0.6, 0.5 and 0.3 mm, respectively. To ensure the accuracy of the interface description, the grid size in the zone with a distance of 2 mm (the size of the liquid inlet boundary) from the wall should be fine in the work. The grid sizes in the location of the interface are 0.1 mm _ 0.6 mm for grid 49 _ 250, 0.05 mm _ 0.6 mm for grid 71 _ 300, 0.05 mm _ 0.3 mm for grid 71 _ 300, and 0.04 mm _ 0.3 mm for grid 81 _ 500. The

interface velocity profiles and average velocity values with four grids are presented in Figs.1. 2 and 1.3. It can be observed that the grid size of 71 _ 500 is finer enough for calculation by considering the computational accuracy and cost. The CFD software, FLUENT, is used to simulate the unsteady film flow. To judge whether the steady state is achieved, the velocities.

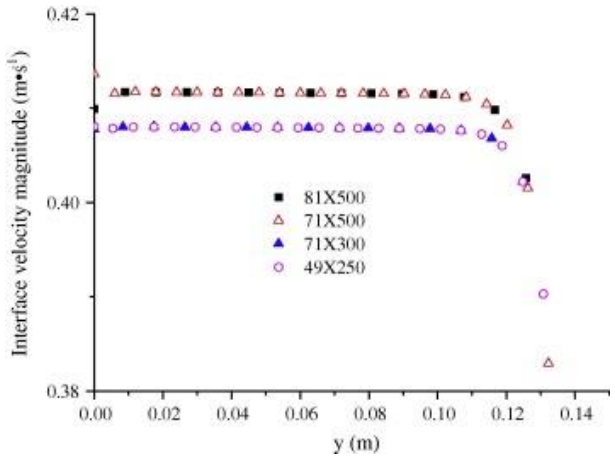

Fig 1.2 Interface velocity magnitude with four types of grids.

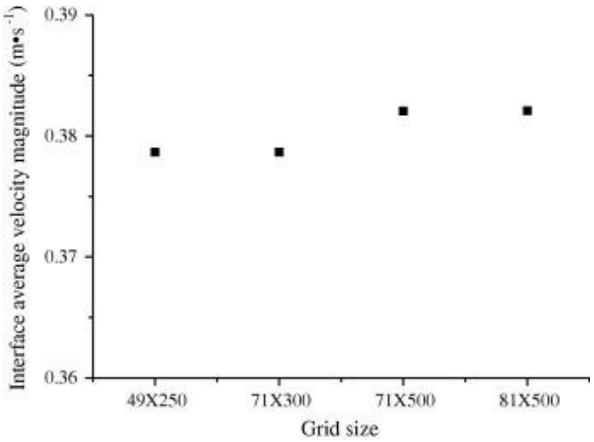

Fig 1.3 Interface average velocity magnitude with four types of grids

II. RESULTS AND DISCUSSION

2.1. VELOCITY PROFILE

The local velocity profile has great influence on the residence time of the liquid and gas phases, which render it a critical factor for the heat and mass transfer process in the dehumidifier. In the
section, the velocity profile of the channel is analyzed. Taking the cross section of the channel at y = 75 mm as an example, as shown in Fig. 1.4

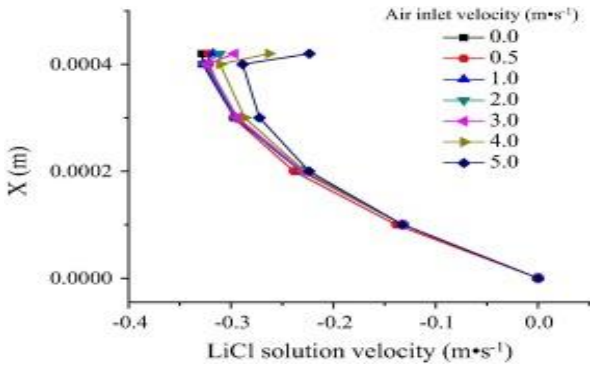

Fig 1.4

The velocity profiles of LiCl solution under different air inlet velocities are presented. In this paper, the LiCl solution flow and air flow are in a counter-current configuration, thus the velocity of the LiCl solution is negative when the velocity of the air is set as positive. When there is not reverse air flow, the velocity of the LiCl solution shows a semi-parabolic distribution, which increases gradually from the plate surface to the gas–liquid interface. The velocity near the plate is zero for the no-slip boundary condition and there is a peak velocity at the gas–liquid interface. If the air flows counter-currently to the LiCl solution with different velocities, the velocity magnitude of the LiCl solution will increase and then decrease, resulting from the drag force of the reversed flow air. With the increase of the air inlet velocity, the influence of the drag force becomes more and more evident, especially when the air inlet velocity reaches more than 3.0 m s_1.

Fig. 1.5 Indicates the velocity profiles of the gas phase. As the liquid and gas phases share the same velocity field in the model, the velocities of the air and LiCl solution are the same at the interface.

When the air inlet velocity is zero, the air near the interphase flows at the same direction with the solution under the function of drag force. It is also found that when the air inlet velocity increases
to some point around 3.0 m s_1, the air becomes the dominated factor to decide the velocity field at the interface and its velocity is no longer following the same direction with the LiCl solution.

4.2. Minimum liquid flow rate for wetting the whole surface Film breakdown of the falling film flow reduces the contact surface of mass transfer during the dehumidification process, thus it
should be avoided as far as possible. It is verified that the critical breakdown point has strong relationship with the liquid flow rate. In this section, the simulation is to make certain the lowest liquid flow rate at which the plate will be fully covered.

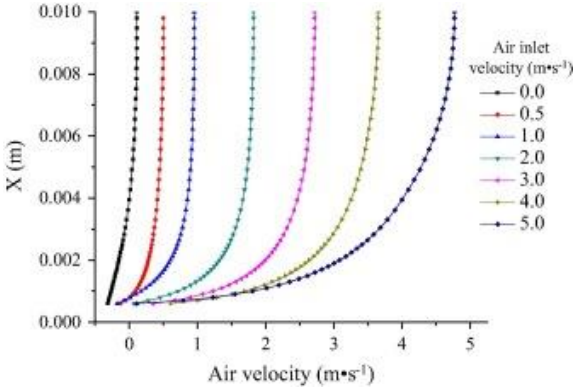

Fig 1.5

In Fig. 1.6, the stages of film formation during solution flow on a flat plate at different liquid flow rates are reported in detail. Testing the flow with the increase of liquid flow rate (operating conditions from No. 1 to No. 4), it is found that the theoretical minimum liquid flow rate to cover the whole plate is about 108.0 m3 m_2 h_1 for the LiCl solution. At the flow rate of 100.8 m3 m_2 h_1, the liquid solution flows in a continuous film at the beginning. Then, the liquid congregates in the liquid film forepart under the function of the surface tension and viscous force. To a certain point, the film would break up under the action of the gravity. It seems that the film rupture occurs at the bottom part of the channel cyclically. Thus, it is difficult to form continuous film at the liquid flow rate of 100.8 m3 m_2 h_1, not to mention lower liquid flow rates. The reason is that the LiCl solution has very high surface tension and contact angle, both of which reduce its wettability significantly. It is observed the air flow rate also has impact on the wetting conditions, especially when the air flows with relatively high velocity.

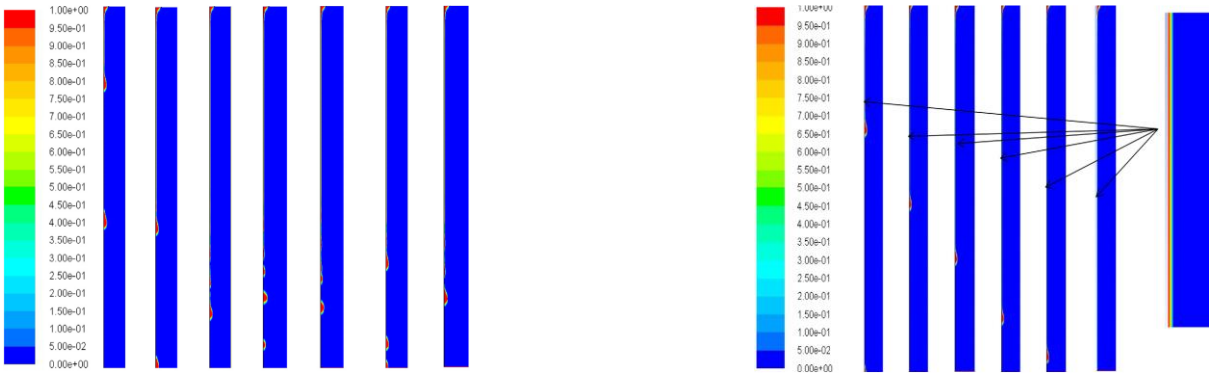

Fig1.6 a)Liquid flow rate: 100.8 m3•m-2•h-1 (Operating condition No. 2) b)Liquid flow rate: 108.0 m3•m-2•h-1 (Operating condition No. 3)

Keeping the LiCl solution flow rate at a constant value of 108.0 m3 m_2 h_1 and increasing the air flow rate from the operating condition No. 5 to No. 7, it is found that when the gas flow rate is up to 21,600 m3 m_2 h_1, some liquid is torn to pieces, as shown in Fig. 1.7. The case must be avoided as the liquid drop carried over by the air will pollute the indoor environment. Under this condition, to wet the whole surface, the LiCl solution flow rate should be increased to 180.0 m3 m_2 h_1 according to the calculation results of the operating condition No. 9.To analyze the influence of the physical properties of the desiccant solution further, an ordinary organic desiccant triethylene glycol (TEG) is chosen for comparison with LiCl solution.

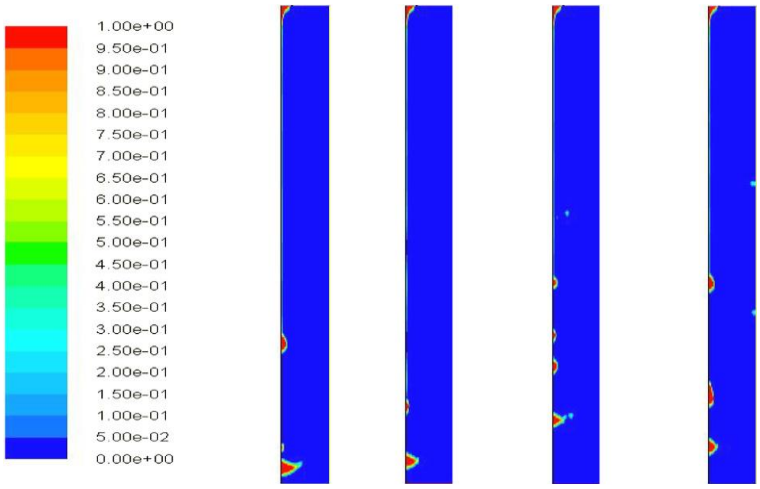

Fig. 1.7.Stages of film formation during solution flow on a flat plate (Operating condition No. 7).

According to the calculation results, it is surprisingly found that even at very low liquid flow rate, the TEG can wet the whole plate surface because the TEG solution has very high viscosity and relatively lower contact angle with the surface. In the flow process, the viscous force and surface tension can resist the gravity, which is the main factor causing the liquid film rupture. However, compared with LiCl solution, it costs much longer time for the TEG solution running through the channel (1.18 s Vs 2.54 s) at the same test condition.

2.2. INTERFACIAL AREA

In this section, the ratio of the interfacial area to the geometrical plate surface as a function of the liquid flow rate is determined. It is noted that the cross section of the flat is the same in the twodimensional calculations, so the ratio can be obtained. The result is demonstrated in Fig. 1.8. Due to the large gas flow rate, it requires that the solution flow rate reaches certain value to wet the whole surface of the flat. Thus, when the solution flow rate is low, the ratio of the interfacial area to the geometrical plate surface is less than one. With the increase of the liquid flow rate, the efficient mass transfer area will increase correspondingly. In some cases, the interfacial area can be larger than the plate because of the wave. As the length of the flat plate is only 150 mm, the effective interfacial area is a little bigger than the geometrical plate surface.However, the increased transfer area can be considerable when the plate is longer and there are lots of plates, which is the real situation of the dehumidifier. Meanwhile, it is also found that when the liquid flow rate achieves a certain value, the increase of the interfacial area will not be obvious anymore.

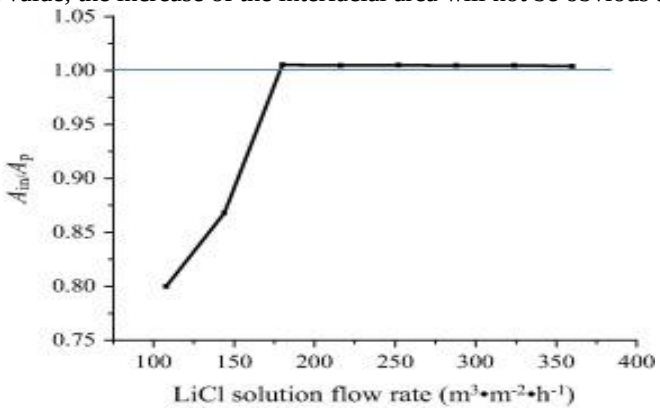

Fig. 1.8.The ratio of the interfacial area to the geometrical plate surface under different liquid flow

2.2. Film thickness

Film thickness is another important parameter investigated in the paper. From Fig. 1.9, it is concluded that with the increase of the liquid flow rate, the average film thickness increases accordingly (air flow rate is 18,000 m3 m_2 h_1). In Fig. 1.9, it is found that the average film thicknesses of present work are a litter bigger than those of the Nusselt empirical formula. It might be resulted from the reverse flow of the air. The local film thickness is presented in Fig. 1.10. It can be observed that the fluctuation amplitude increases continuously in the liquid flow direction. The fluctuation amplitude also rises when the liquid flow rate increases, which explains the increased
interface area mentioned in Section 4.3. Thus, the fluctuation is beneficial to mass transfer in the aspect. Except for the interface area, the further research about how the fluctuation affects the
mass transfer is needed.

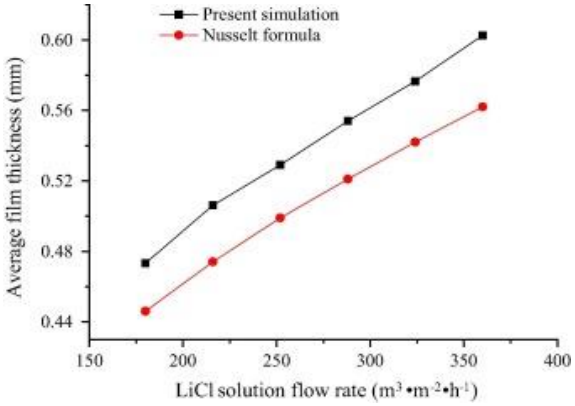

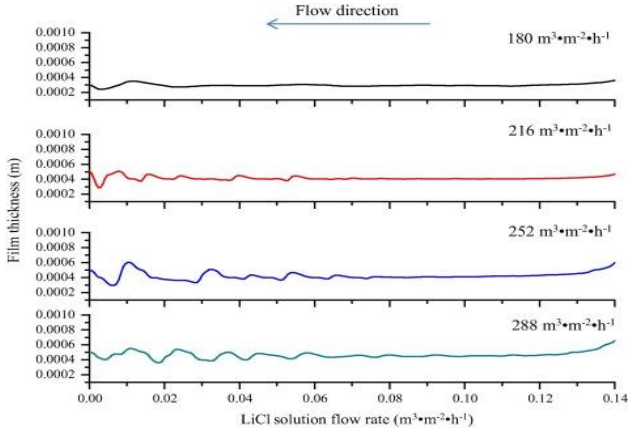

Fig. 1.9.Average film thickness at different LiCl solution flow rates. **Fig. 1.10**.Liquid film thickness profiles at Different LiCl solution flow rates.

III. CONCLUSION

Based on the calculation results, it is concluded that the simulation model can predicate the dynamic and local flow conditions in the dehumidifier interior microscopically.

The velocity profiles in the dehumidifier are demonstrated. It is found that the counter-flow air does change the velocity profile of the LiCl solution along the film thickness due to the drag force. And when the air inlet velocity reaches 3.0 m s_1, the impact becomes very distinct. Under that situation, the air becomes the dominated factor to decide the velocity field at the interface.With the model, the importance of suitable solution and air flow rates can be highlighted.

According to the simulation results, it has been found that if the solution flow rate is too low, the effective interfacial area can be reduced significantly due to the film breakdown. If the air flow rate is too high, it is possible for the air to carry over the liquid drop, which will be a big threaten to
the indoor environment. Therefore, the model can be an effective way to predicate the optimum flow rates of the solution and air in advance.

The results also explain the reason of the enhancement of mass transfer with film flow. It is because with the increase of the liquid flow rate, the fluctuation amplitude and the efficient mass transfer area will increase correspondingly. In some cases, the interfacial area can be larger than the plate because of the wave. And the increased transfer area can be considerable when the plate area is large enough. In this way, the mass transfer in the film flow absorber can be improved significantly.

In the future work, the impact of the film fluctuation on the absorption performance of the dehumidifier will be investigated in depth.

IV REFERENCES:

[1] Oberg V, Goswami DY. Experimental study of the heat and mass transfer in a packed bed liquid desiccant air dehumidifier. J Sol Energy Eng 1998;120:289–97.

[2] Potnis SV, Lenz TG. Dimensionless mass-transfer correlations for packed-bed liquid desiccant contactors. Ind Eng Chem Res 1996;35(11):4185–93.

[3] Oberg V, Goswami DY. Advances in solar energy: an annual review of research and development. American Solar Energy Society Inc.; 1998. 12: p. 431–70.

[4] Xie XY, Jiang Y, Tang YD, Yi XQ, Liu SQ. Simulation and experimental analysis of a fresh air-handling unit with liquid desiccant sensible and latent heat recovery. Build Simul 2008;1:53–63.

[5] Rix J, Nevrala D, Chauvet L, Probert SD. Gas-powered liquid desiccant dehumidifier. Appl Energy 1993;45:167–80.

[6] Xiao F, Ge GM, Niu XF. Control performance of a dedicated outdoor air system adopting liquid desiccant dehumidification. Appl Energy 2011;88:143–9.

[7] Xiong ZQ, Dai YJ, Wang RZ. Development of a novel two-stage liquid desiccant dehumidification system assisted by CaCl2 solution using exergy analysis method. Appl Energy 2010;87:1495–504.

[8] Audah N, Ghaddar N, Ghali K. Optimized solar-powered liquid desiccant system to supply building fresh water and cooling needs. Appl Energy 2011;88:3726–36.

[9] Colinet P, Legros JC, Velarde MG. Nonlinear dynamics of surface-tension-driven instabilities. New York: Wiley-VCH; 2001. p. 512.

[10] Grossman G. Simultaneous heat and mass transfer in film absorption under laminar flow. Int J Heat Mass Transfer 1983;26(3):357–71.

[11] Grossman G. Simultaneous heat and mass transfer in absorption of gases in turbulent liquid films. Int J Heat Mass Transfer 1984;27(12):2365–76.

[12] Luo YM, Yang HX, Lu L. Liquid desiccant dehumidifier: Development of a new performance predication model based on CFD. Int J Heat Mass Transfer 2014;69:408–16.
[13] Luo YM, Shao SQ, Xu HB, Tian CQ. Dehumidification performance of [EMIM]BF4. Appl Therm Eng 2011;31(14–15):2772–7.
[14] Luo YM, Shao SQ, Qin F, Tian CQ, Yang HX. Investigation of feasibility of ionic liquids used in solar liquid desiccant air conditioning system. Sol Energy 2012;86:2718–24.
[15] Luo YM, Yang HX, Lu L, Qi RH. A review of the mathematical models for predicting the heat and masstransfer process in the liquid desiccant dehumidifier. Renew Sust Energ Rev 2014;31:587–99.
[16] Khosravi Nikou MR, Ehsani MR. Turbulence models application on CFD simulation of hydrodynamics, heat and mass transfer in a structured packing. Int Commun Heat Mass 2008;35:1211–9.
[17] Haelssig JB, Tremblay AY, Thibault J, Etemad SG. Direct numerical simulation of interphase heat and mass transfer in multicomponent vapour-liquid flows. Int J Heat Mass Transfer 2010;53:3947–60.
[18] Haroun Y, Raynal L, Legender D. Mass transfer and liquid hold-up determination in structured packing by CFD. Chem Eng Sci 2012;75:342–8.
[19] Ansys Fluent User's Guide 13.0.
[20] Brackbill JU, Kothe PB, Zemach C. A continuum method for modeling surface tension. J. Comput Phys. 1992;100:335–54.